11th Australasian Fluid Mechanics Conference
University of Tasmania, Hobart, Australia
14-18 December 1992

UNSTEADY CHARACTERISTICS OF FLUID FLOW AND HEAT TRANSFER ON A SEPARATED REGION OF A CIRCULAR CYLINDER

Masaya KUMADA[1], Masataka KATO[2], Sadao FUJITA[3] and Teruaki MITSUYA[4]

[1]Dept Mechanical Engineering, Gifu University, 1-1 Yanagido, Gifu 501-11, JAPAN

[2]Toyo Denki Co Ltd, 1-39 Kagiya, Kasugai 480, JAPAN

[3]Aisin Seiki Co Ltd, 1 Asahi-machi, Kariya 448, JAPAN

[4]Hitachi Research Laboratory, 402b Kuji-cho, Hitachi 319-12, JAPAN

ABSTRACT

To clarify the mechanism of fluid flow and heat transfer in a near wake region of a circular cylinder in a uniform cross-flow, unsteady and 3-dimensional characteristics of the flow field and the heat transfer were measured using the flow direction probes for instantaneous velocity and flow direction and small dynamic heat flux sensors for the instantaneous heat transfer coefficients of the axial direction and around the circumference. These data are processed under the condition of the frequency of Karman vortex shedding. The flow field in the separated region of a circular cylinder can be divided into three regions: (1) $160^\circ \leqq \theta$, the alternative boundary layer flow interlocked with Karman vortex shedding, (2) $130^\circ \leqq \theta < 160^\circ$, the region affected by the concentration of the vortex and Karman vortex shedding, and (3) $78^\circ \leqq \theta < 130^\circ$, the region governed by the entrainment flow of a separated shear flow. In the region of (1), the streamwise flow is accelerated and the reverse flow is decelerated. Three-dimensionality of the axial direction is shown by the characteristic length, which is one cylinder diameter in the range of this study.

NOMENCLATURE

d : cylinder diameter
f : frequency
h : instantaneous heat transfer coefficient
PH : phase
Re : reynolds number=Ud/ ν
Sv : output of sensor wire
U : mean velocity
u : velocity
u' : fluctuating velocity
X : distance of streamwise direction
Y : distance of radial direction of cylinder
Z : distance of axial direction of cylinder
θ : angle
τ : time

Subscript
($\overline{\ }$): phase mean

INTRODUCTION

In order to clarify the mechanism of flow field and heat transfer in a separated region of a circular cylinder in a uniform crossflow, many investigations covering a wide range of Reynolds number have been performed over a long period of time. Recently, with the development of computers and techniques of flow visualization, useful results of these problems at low Reynolds number have been obtained numerically and qualitatively. However, in the region of high Reynolds number, information in the near-wake region has still not been clarified, because the flow field is unsteady and exhibits 3-dimensional behavior. Therefore, accumulation of time and partial data is indispensable.

Unfortunately, a hot wire anemometer is not available for the flow field where the instantaneous flow direction will change, and as described in many papers (Jones,1977), there are few effectual sensors which can be applied to the partial measurement of the heat transfer coefficient described above. This is due not only to sensitivity but also to space resolution.

Conventionally, some studies (Williamson, 1989; Yokoi and Kamemoto, 1991) have reported on the 3-dimensional behavior of the flow field. They discussed the relationship between the boundary separation and the separated shear flow in the wake region of the circular cylinder. However, no studies have been performed to show the relationship between the 3-dimensional flow structure and the heat transfer mechanism.

On the other hand, models of the heat transfer mechanism in the separated region were proposed by Igarashi and Hirata (1973) and Sano and Nishikawa (1964). However, these models were based on results of time-averaged heat transfer coefficients around the circumference. They took the periodic shedding of Karman vortex into consideration, but were not verified with experimental results of the flow field.

On the basis of these results, in this report, two measurement techniques were improved and developed for fluid flow and heat transfer. One is a flow direction probe (Westphal et al, 1981) to determine the instantaneous velocity and flow direction. The other is a small dynamic heat flux sensor (Kawamura et al, 1987) to determine the instantaneous heat transfer coefficient. We accumulated the instantaneous heat transfer distributions of the axial direction and around the circumference. These data are processed under the condition of the frequency of Karman vortex shedding. On the basis of these data, we investigated the instantaneous relationship between the flow field and heat transfer distribution.

EXPERIMENTAL APPARATUS AND PROCEDURES

The wind tunnel used in this study was a blow-down type with a working section of 0.3-m x 0.4-m cross-sectional area and 2-m length. The tests were performed at a free-stream velocity U=9-15 m/s; Reynolds number=(2.28-3.66)x10^4.

Figure 1 is a schematic diagram of the flow direction probe in pairs mounted in the circular cylinder. The central wire (tungsten, 5 μ m diameter) was heated using the same principle as the constant-temperature hot-wire anemometer. The temperature-sensing wires, located in front of and behind the heating wire, were made of tungsten and 5 μ m in diameter. These three wires can be moved precisely and independently of each other in the vertical direction of the wall surface, using a rack-and-pinion device. The instantaneous flow direction was determined by the output signal of the sensor wire. Flow direction probes can be moved around the circumference.

Figure 2 is a schematic diagram of the heat transfer cylinder used for measuring the heat transfer coefficient around the circumference of a cylinder. The measured part of the cylinder is made of copper and both ends of the cylinder are made of bakelite. The cylinder diameter is 40-mm. The aspect ratio and blockage ratio are 7.5 and 0.1, respectively. The cylinder was heated with the sheath heater, as shown in

the figure. The cylinder for measuring the axial direction is of the same construction as that shown in Fig. 2.

The heat flux meters were controlled at a constant temperature by temperature-feedback amplifiers, using the same principle as the constant-temperature hot-wire anemometer. As shown in Fig. 2, 18 dynamic heat flux meter sensors were arrayed on the heat transfer surface. Figure3 shows the pattern of a dynamic heat flux sensor. The nickel film heater (3 μ m thick), which also functions as a surface temperature sensor, was attached to a copper block with two-sided adhesive tape. The film was formed into the pattern by a chemical etching process. The temperature-compensating register, which forms a part of a Wheatstone bridge, was adhered to a side surface of a copper block to equilibrate the film temperature accurately with temperature of the surrounding heat transfer surface. The controlling circuit is the same as that used in the experiment of the previous report (Kawamura et al,1987). Static calibration of the dynamic heat flux meter was performed during stagnation heat transfer on a cylinder. Dynamic calibration of the heat fluxmeter was performed under the same conditions as for static calibration with pulsative light radiation. The light pulse was projected from a halogen lamp(400 W) and cut by a rotating drum shutter with multiple rectangular windows to an on/off ratio of 1:1. The amplitude at 150 Hz was about half that in the constant-amplitude region (f< 25 Hz). Thus the time constant for the response of the dynamic heat flux meter, including the constant-temperature controller, was estimated to be about 2.1 ms.

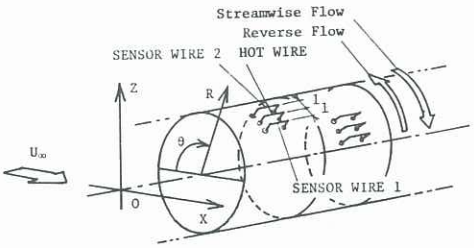

Fig.1 Flow direction probe

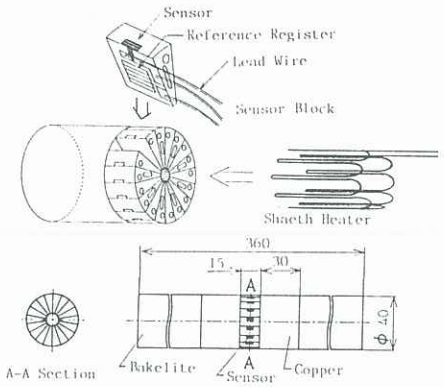

Fig.2 Heat transfer cylinder

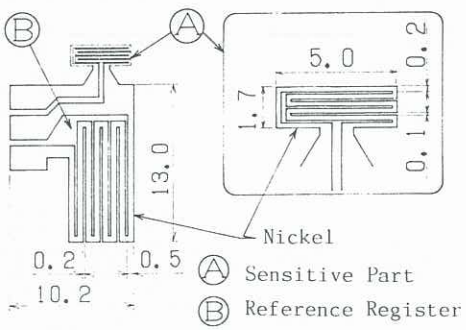

Fig.3 Pattern of dynamic heat flux sensor

RESULTS AND DISCUSSION

Characteristics of flow field

Results of frequency analysis of the hot-wire signal and sensor wire signal of the flow direction probe are shown in Figs. 4(a) and (b). The frequency of Karman vortex shedding is 100 Hz at this experimental velocity. Comparing the two figures, $\theta \leqq 130^\circ$, we find that neither shows the peak at a specified frequency. This corresponds to the secondary vortex region discussed by Boulos and Pei(1974) and to the hump region appearing in the heat transfer distribution in the case (Mabuchi et al, 1974) of a splitter plate inserted into the wake region. When $\theta \geqq 140^\circ$, the output of the sensor wire shows a peak only at 100 Hz. This means the change of the flow direction interlocks the shedding of the Karman vortex. Conversely, results of the hot-wire signal show the peak at the double frequency (200 Hz) of Karman vortex shedding in the case of $\theta = 180^\circ$ and two peaks, at the shedding frequency (100 Hz) and the double frequency (200 Hz), in the case of $\theta = 170^\circ$. Then, when $\theta \leqq 160^\circ$, the peak is shown only at 100 Hz. This means that flow is not induced by vortex formation from upstream of $\theta = 160^\circ$ to downstream. In fact, at $\theta \leqq 160^\circ$, the catching ratio of streamwise flow by the flow direction probe is less than one-half of that of reverse flow, but $80^\circ \leqq \theta \leqq 130^\circ$, both catching ratios are of the same order.

Output of the hot-wire of the flow direction probe has high frequency of turbulence in addition to the frequency of Karman vortex shedding, as shown in Fig. 5. In order to analyze the change of velocity in a periodic time of Karman vortex shedding, data were processed by computer after smoothing and dividing into 16 phases in a periodic time. As shown in this figure, the high frequency component defined by the relation of u'=U-u does not have a specified frequency. In the frequency distribution of velocity in each phase, their variances gradually increase as θ increases. This reflects on

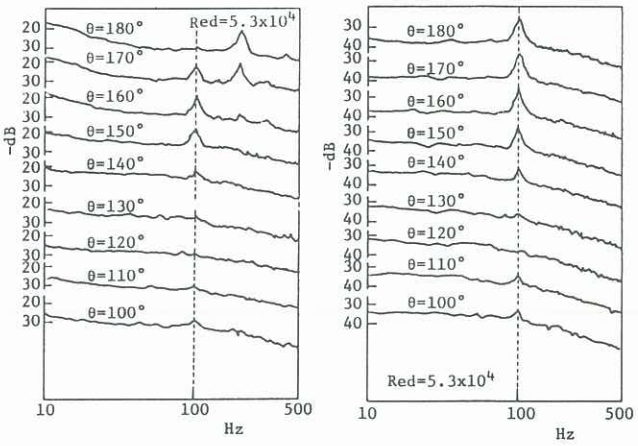

Fig.4(a) Hot-wire signal

Fig.4(b) Sensor-wire signal

Fig.4 Frequency analysis

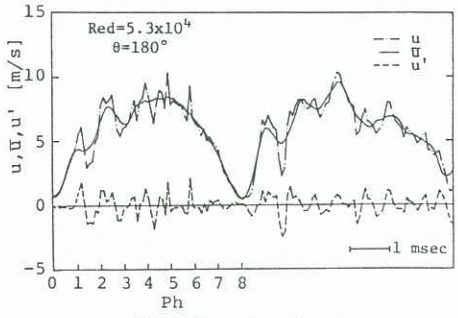

Fig.5 Hot-wire signal

the entrainment flow being covered in this region ($140^\circ < \theta \leqq 180^\circ$) while a vortex is formed and shed. Figure 6 shows changes in the arithmetical mean velocity of each phase during a periodic time. Generally, reverse flow is larger than streamwise flow, regardless of θ. Furthermore, the flow changes from streamwise flow to reverse flow as a sine wave and alternately accelerates and decelerates. Both flows show the maximum velocity at the central phase.

Figure 7 shows examples of changes in the radial direction distribution of mean velocity at each phase. The distributions at each phase are similar to the boundary layer velocity profile.

Characteristics of instantaneous heat transfer

At first, it was confirmed that the distributions of total time-averaged heat transfer coefficients with respect to θ agreed very well with the conventional results. Furthermore, the mean value, which numerically integrates this distribution over all angles, agreed fairly well with the result of McAdams (1954).

The result of frequency analysis of a dynamic heat flux sensor's output signal is shown in Fig. 8. The frequency characteristic of the sensor signal agrees well with that of the hotwire signal, as shown in Fig. 4(a). Therefore, this suggests that instantaneous heat transfer coefficients in the separated region become large due to the effect of periodic thermal boundary layer renewal caused by the alternative boundary layer flow formed near the wall, interlocking with the frequency of Karman vortex shedding.

Considering the above result, all signals of sensors were measured simultaneously with the signal of the hotwire which was inserted downstream of the cylinder and by which the waveform of velocity fluctuation due to Karman vortex shedding was measured.

Figure 9 shows the axial distribution of the phase-mean heat transfer coefficients around $\theta = 80^\circ$. As described conventionally, the value around the separated point changes periodically, not only within one periodic time but also in the axial direction.

Figure 10 shows the axial distribution of the phase-mean value at the rear stagnation point ($\theta = 180^\circ$) within one periodic time. As shown in Fig. 8, h at $\theta = 180^\circ$ changes with a period of the double frequency of Karman vortex shedding. Furthermore, even if $\bar{h}$ is the averaged value of each phase, a change in axial direction is observed.

As described in a series of figures of the phase-aver-

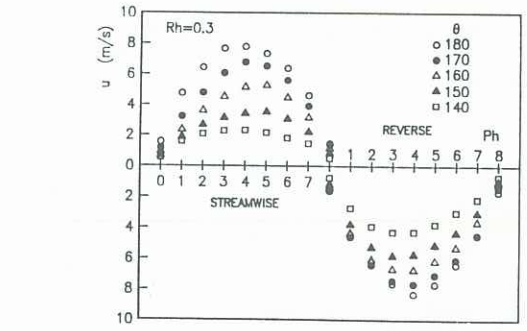

Fig.6 Phase mean velocity

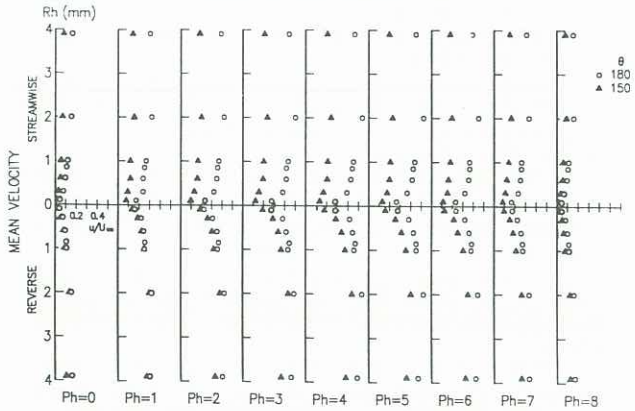

Fig.7 Radial direction distribution of mean velocity

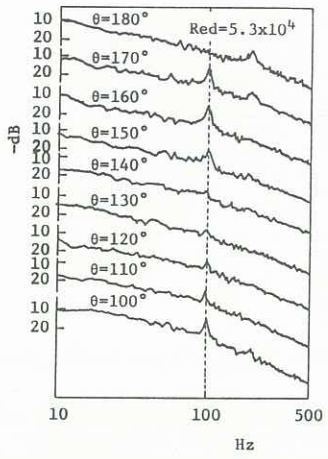

Fig.8 Frequency analysis of heat flux sensor signal

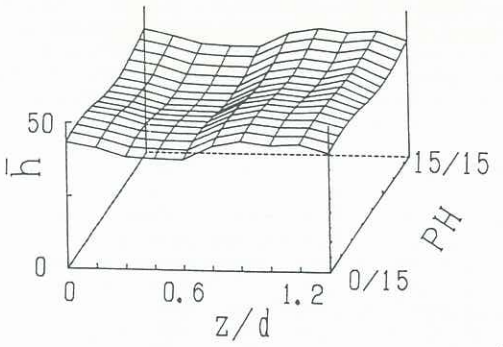

Fig.9 Axial distribution of h at $\theta = 80^\circ$ ($Re = 2.28 \times 10^4$)

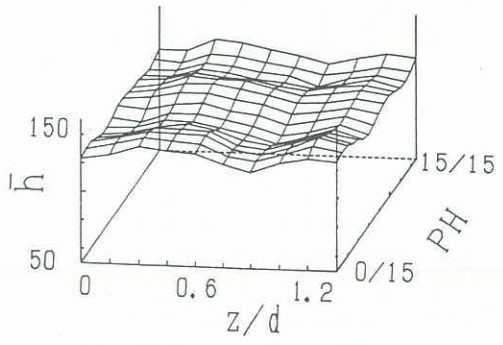

Fig.10 Axial distribution of h at $\theta = 180^\circ$ ($Re = 3.66 \times 10^4$)

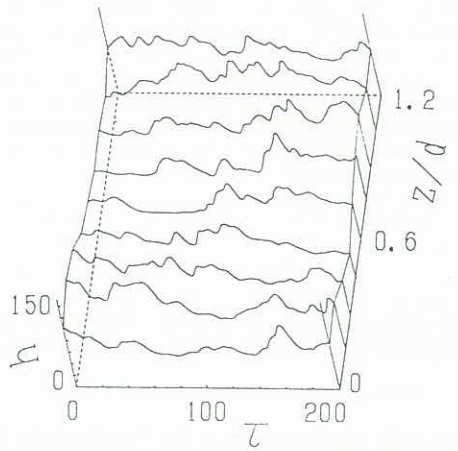

Fig.11 Time change of h in axial direction ($\theta = 180^\circ$)

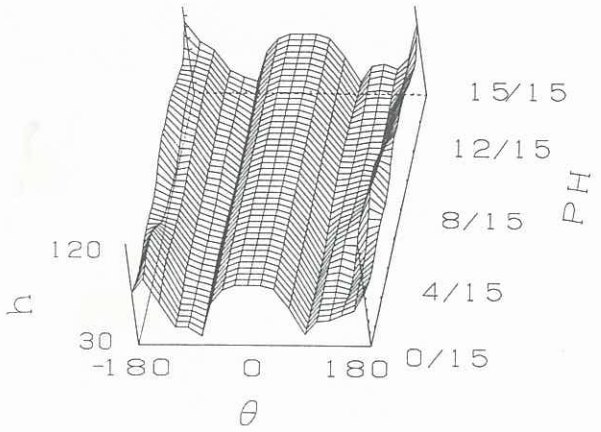

Fig.12 Time change of h around the cylinder

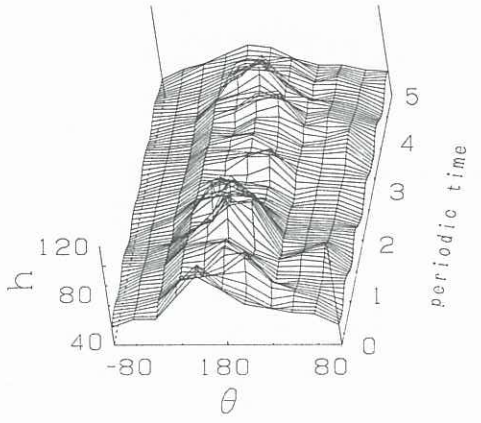

Fig.13 Time change of h in the separated region

aged value, $\bar{h}$ changes in the axial direction. It can be considered that there is an effect of 3-dimensionality of the flow, and this means that the separated shear flow has three-dimensional behavior. Figure 11 shows the time change of instantaneous heat transfer coefficients at $\theta = 180^\circ$. As shown in this figure, the peak value of the output waveform moves in the axial direction with a given period of timelag. Furthermore, it seems that the movement is not monotonous but discontinuous. As the measuring distance is insufficient, it is not clear whether the same behavior is repeated periodically or not, but it seems that the moving behavior has a certain wavelength; that is, it is equal to about one diameter of the cylinder in this experiment. The measurement should be done again, using a cylinder with a different diameter. However, it is very important that this value be on the extension of the line given Yokoi and Kamemoto (1991) who obtained the result using the flow visualization technique in the range of Reynolds numbers from 170 to 1340.

Figure 12 shows the time change of local instantaneous heat transfer coefficients around the circumference. Nothing has been reported, so far as the authors have determined from the literature, about this kind of result. As expected, the heat transfer in the region of the laminar boundary layer is extremely stable, and there is a symmetry about the front stagnation point. However, in the separated region, the effect of Karman vortex formation is very complicated and the heat transfer mechanism is intricate; for example, the maximum value of h is not always at the rear stagnation point. In order to discuss the heat transfer behavior in detail, the time change of local instantaneous heat transfer coefficients in the separated region is shown in Fig. 13. As shown in this figure, the region of $-160^\circ \leqq \theta \leqq +160^\circ$ and the region of $+80^\circ \leqq \theta < +160^\circ$ ($-80^\circ \leqq \theta < -160^\circ$) are extremely different in their degrees of fluctuation. In $-160^\circ \leqq \theta \leqq +160^\circ$, the maximum value moves from $\theta = +160^\circ$ to $\theta = -160^\circ$ through $\theta = 180^\circ$ with time, and then moves from $\theta = -160^\circ$ to $\theta = +160^\circ$ through $\theta = 180^\circ$ with time. According to the result of the phase-mean value, it crosses the point of $\theta = 180^\circ$ twice within one periodic time. This can also be explained in terms of the result of frequency analysis (Fig. 8). Thus, in interlocking with the frequency of Karman vortex shedding, the alternative boundary layer flow is formed on the wall near the rear stagnation point.This experimental result conflicts with the model of the rear stagnation flow (Igarashi and Hirata, 1973).

On the other hand, in $+80^\circ \leqq \theta < +160^\circ$, it seems that the fluctuation of h is small and has constant periodicity. As shown in Fig.11, the distribution of h shows the hump in $+80^\circ \leqq \theta \leqq +130^\circ$. This may be explained by the effect of the separated shear flow, that is the vortex concentration due to the development of the shear layer. However, the behavior in the region of $+130^\circ < \theta < +160^\circ$ is not clarified.

CONCLUSIONS

Unsteady characteristics of the flow field and time series data of the instantaneous heat transfer coefficient were accumulated. A summary of the results and considerations follows.

(1) Flow field in the separated region of a circular cylinder can be divided into three regions; that is,
   ①$160^\circ \leqq \theta$, the alternative boundary layer flow interlocked with the frequency of Karman vortex shedding,
   ②$130^\circ \leqq \theta < 160^\circ$, the region affected by concentration of vortex and Karman vortex shedding.
   ③$78^\circ \leqq \theta < 130^\circ$, the region governed by the entrainment flow of a separated shear flow.
(2) In the region of ①, the streamwise flow is accelerated and the reverse flow is decelerated.
(3) Three-dimensionality of axial direction is shown by the characteristic length, which is one cylinder diameter in this experiment.
(4) The peak of instantaneous heat transfer coefficients moves from $\theta = +160^\circ$ to $\theta = -160^\circ$ through $\theta = 180^\circ$ and then moves again. This movement is repeated with the frequency of Karman vortex shedding.
(5) Close agreement between the characteristics of fluid flow and heat transfer was obtained.

REFERENCES

BOULOS,MI and PEI,DCT(1974) Dynamics of heat transfer from cylinders in a turbulent air stream.Int.J. Heat Mass Transfer, 17, 767-783.

IGARASHI,T and HIRATA,M (1973)Heat transfer in sepa-rated flows. Trans Japan Soc Mech Eng, 39, 1890-1889 (in Japanese).

JONES,TV(1977) Measurement of unsteady fluid dynamic phenomena. BE Richards,ed., Hemisphere Publishing, Washington, 63-121.

KAWAMURA,T, TANAKA,S, MABUCHI,I and KUMADA,M (1987-1988) Temporal and spatial characteristics of heat transfer at the reattachment region of a backward-facing step. Experimental heat transfer, 1, 299-313.

MABUCHI,I, HIWADA,M and KUMADA,M (1974) Some experiments associated with heat transfer mechanism. Proc 5th Int. Heat Transfer Conf. Tokyo, FC8.5, 315-319.

MCADAMS,WH (1954) Heat Transmission, McGraw-Hill, 3rd. ed., 259-260.

SANO,Y and NISHIKAWA,S(1964) Analysis of heat transfer of a cylinder in cross flow fluid by the intermittent penetration theory. Kagaku kougaku (Chemical engineering), 28, 956-960 (in Japanese).

YOKOI,Y and KAMEMOTO,K(1991)The initial stage of a three-dimensional vortex structure existing in a two-dimensional boundary layer separation flow. Trans Japan Soc Mech Eng, 57, 427-433 (in Japanese).

WESTPHAL,RV, EATON,JK and JOHNSON,TR (1981) A new probe for measurement of velocity and wall shear stress in unsteady, reversing flow. Trans. ASME, 91, 478-482.

WILLIAMSON,CHK(1989) Oblique and parallel modes of vortex shedding in the wake of a circular cylinder at low Reynolds numbers. J. Fluid Mech, 206, 579-627.